AGU PUBLICATIONS

Geochemistry, Geophysics, Geosystems

RESEARCH ARTICLE
10.1002/2014GC005528

Key Points:
- The deep proto-North Atlantic was completely anoxic during OAE2
- Redox proxies reveal spatial differences in bottom water redox conditions
- Bottom water circulation in the basin was severely restricted

Supporting Information:
- Readme
- Figure S1
- Table S1

Correspondence to:
N. A. G. M. van Helmond,
n.vanhelmond@uu.nl

Citation:
van Helmond, N. A. G. M., I. Ruvalcaba Baroni, A. Sluijs, J. S. Sinninghe Damsté, and C. P. Slomp (2014), Spatial extent and degree of oxygen depletion in the deep proto-North Atlantic basin during Oceanic Anoxic Event 2, *Geochem. Geophys. Geosyst.*, *15*, 4254–4266, doi:10.1002/2014GC005528.

Received 28 JUL 2014
Accepted 16 OCT 2014
Accepted article online 23 OCT 2014
Published online 11 NOV 2014

Spatial extent and degree of oxygen depletion in the deep proto-North Atlantic basin during Oceanic Anoxic Event 2

Niels A. G. M. van Helmond[1], Itzel Ruvalcaba Baroni[2], Appy Sluijs[1], Jaap S. Sinninghe Damsté[2,3], and Caroline P. Slomp[2]

[1]Faculty of Geosciences, Laboratory of Palaeobotany and Palynology, Department of Earth Sciences, Utrecht University, Utrecht, Netherlands, [2]Faculty of Geosciences, Department of Earth Sciences, Utrecht University, Utrecht, Netherlands, [3]NIOZ Royal Netherlands Institute for Sea Research, Texel, Netherlands

Abstract Massive organic matter burial due to widespread ocean anoxia across the Cenomanian/Turonian boundary event (~94 Ma) resulted in a major perturbation of the global carbon cycle: the so-called Oceanic Anoxic Event 2 (OAE2). The characteristics and spatial distribution of the OAE2 deposits that formed in the deep basin of the proto-North Atlantic remain poorly described, however. Here we present proxy data of redox sensitive (trace) elements (e.g., Mo, Fe/Al, C_{org}/P_{tot}, and Mn) for OAE2 sediments from five Deep Sea Drilling Project and Ocean Drilling Program sites located in the deep proto-North Atlantic basin. Our results highlight that bottom waters in the entire deep proto-North Atlantic were anoxic during most of OAE2. Furthermore, regressions of Mo with total organic carbon content (TOC), previously shown to document the degree of water mass restriction, confirm that the water circulation in the proto-North Atlantic basin was severely restricted during OAE2. Comparison of these values to Mo/TOC ratios in the present-day Black Sea suggests a renewal frequency of the deep proto-North Atlantic water mass of between 0.5 and 4 ka, compared to a maximum of ~200 years for the present-day northern Atlantic. The Plenus Cold Event, a cooler episode during the early stages of OAE2 hypothesized to be caused by declining pCO_2 due to extensive burial of organic matter, appears to have led to temporary re-oxygenation of the bottom water in the deep proto-North Atlantic basin during OAE2.

1. Introduction

The mid-Cretaceous Cenomanian-Turonian boundary event (CTBE; ~94 Ma) marks the widespread deposition of organic-rich marine sediments associated with large-scale ocean anoxia [*Schlanger and Jenkyns*, 1976; *Arthur and Sageman*, 1994]. Oceanic Anoxic Event 2 (OAE2) is characterized by a positive >2‰ excursion in the stable carbon isotopic composition ($\delta^{13}C$) of the global exogenic carbon pool, recognized in sedimentary organic matter ($\delta^{13}C_{org}$) and carbonate ($\delta^{13}C_{carb}$) [e.g., *Kuypers et al.*, 2002; *Tsikos et al.*, 2004]. The ~600 kyr long [e.g., *Meyers et al.*, 2012] positive carbon isotopic excursion (CIE) typically encompasses three phases, the onset (phase A), a plateau phase with relatively stable values (phase B), and a recovery phase to pre-event values (phase C) [e.g., *Kuypers et al.*, 2004a]. The onset and presumably the plateau phases are most likely the result of enhanced burial of $\delta^{13}C$-depleted organic matter [*Schlanger and Jenkyns*, 1976; *Arthur et al.*, 1988; *Sinninghe Damsté and Köster*, 1998; *Kuypers et al.*, 2002; *Tsikos et al.*, 2004].

OAE2 has been linked to the emplacement of the large igneous province (LIP) of the Caribbean Plateau [*Leckie et al.*, 2002]. The associated release of trace metals to the marine environment, as deduced from enrichments of a wide range of trace metals in sediments [*Snow et al.*, 2005], has been suggested to have fueled primary production in the proto-North Atlantic by reducing trace-metal limitation of nitrogen fixers [*Morel and Price*, 2003; *Trabucho Alexandre et al.*, 2010]. The increased igneous activity [e.g., *Kuroda et al.*, 2007; *Turgeon and Creaser*, 2008] also led to high levels of atmospheric CO_2 [e.g., *Bice et al.*, 2006; *Sinninghe Damsté et al.*, 2008; *Barclay et al.*, 2010], and extreme warmth during OAE2 [e.g., *Forster et al.*, 2007; *Sinninghe Damsté et al.*, 2010]. As a consequence of the warming, oxygen solubility in seawater decreased. In combination with a more stratified water column, this led to a reduced ventilation of the ocean and an expansion of areas of anoxia, and even photic-zone euxinia, i.e., free H_2S in the water column [*Sinninghe Damsté and Köster*, 1998; *Kuypers et al.*, 2002]. The prevailing extreme greenhouse conditions also enhanced the hydrological cycle, which induced freshwater stratification on shelves and in epicontinental seas and led to

enhanced weathering, increasing continentally derived nutrient input and primary productivity [*Pogge von Strandmann et al*., 2013; *van Helmond et al*., 2014]. Once anoxia was established, recycling and upwelling of phosphorus (P) and nitrogen (mostly as NH_4) and fixation of N_2 from the atmosphere further boosted primary productivity [*Kuypers et al*., 2004b; *Mort et al*., 2007; *Kraal et al*., 2010; *Higgins et al*., 2012].

A wide range of proxies can be employed for the reconstruction of redox conditions. The simplest one is the total organic carbon content (TOC) of sediments. However, along with bottom water oxygen conditions, TOC content is also a function of the organic matter flux to the seafloor, degradation of organic matter and dilution with inorganic matter [e.g., *Reed et al*., 2011]. Concentrations of trace metals in sediments, e.g., V, Cr, Cu, Zn, Ni, and in particular Mo [*Brumsack*, 1980; *Emerson and Huested*, 1991; *Scott and Lyons*, 2012] have been shown to be excellent proxies for paleoredox conditions in bottom waters. They are actively scavenged from oxygen-depleted marine environments, and therefore enriched in the sediments. Mn and P, in contrast, are mobilized under reducing conditions. Therefore, depletions in sedimentary Mn [e.g., *Thomson et al*., 1995; *Lenz et al*., 2014] and the ratio of organic carbon over total phosphorus (C_{org}/P_{tot}) [*Algeo and Ingall*, 2007] can be used as an indicator for seafloor deoxygenation. C_{org}/P_{tot} ratios also provide insight in the degree of P recycling [*Mort et al*., 2007; *Kraal et al*., 2010]. An elevated value of Fe/Al ratios is indicative of a sedimentary enrichment of Fe relative to a detrital background. Such enrichments are assumed to be the result of enhanced Fe-shuttling from continental margins to the deep sea, driven by the expansion of low-oxygen zones, thus providing a proxy for more widespread anoxia [e.g., *Canfield et al*., 1996; *Lyons and Severmann*, 2006; *Eckert et al*., 2013]. Additionally, regressions between Mo and TOC can provide insight into the degree of restriction of the subchemoclinical water mass [*Algeo and Lyons*, 2006].

Most sedimentary records for OAE2 have been obtained from continental margins. These records indicate significant temporal and spatial differences in primary productivity and bottom water redox conditions in the coastal zone during the event [e.g., *Tsikos et al*., 2004; *Hetzel et al*., 2011; *van Helmond et al*., 2014]. For example, high total organic carbon (TOC) contents (generally $>$10%), organic carbon over phosphorus ratios (C_{org}/P_{tot}; generally $>$600), and trace-metal contents (e.g., molybdenum; Mo $>$40 parts per million; ppm) are observed on the Moroccan shelf [*Tsikos et al*., 2004; *Kraal et al*., 2010]. In contrast, the European and North American shelves (e.g., New Jersey) are characterized by a low TOC content (generally $<$1%), a low C_{org}/P_{tot} ratio (generally $<$100), and a low trace-metal content (e.g., Mo $<$5 ppm) [*Hetzel et al*., 2011; *van Helmond et al*., 2014]. Bottom water redox conditions in the deep central basin of the proto-North Atlantic, i.e., at estimated water depths $>$2000 m, during OAE2 are less well constrained than at continental margins. Data sets, including TOC content, trace-metal concentrations and C_{org}/P_{tot} ratio are only available for two Deep Sea Drilling Project (DSDP) sites: 367 and 603. DSDP Site 367, which is located in the southern deep part of the proto-North Atlantic, is characterized by an extremely high (i.e., 20–40%) and relatively stable TOC content, high (i.e., 400–1500) C_{org}/P_{tot} ratios, high trace-metal contents (e.g., Mo $>$50 ppm) and high Fe/Al ratios (i.e., 1–3) [*Kuypers et al*., 2002; *Kraal et al*., 2010; *Owens et al*., 2012]. At DSDP Site 603 in the northern deep part of the proto-North Atlantic, in contrast, concentrations and ratios of the same elements for OAE2 are significantly lower and much more variable [*Kuypers et al*., 2004b; *Kraal et al*., 2010; *Owens et al*., 2012]. The lack of further insight in the spatial extent and temporal variability in bottom-water anoxia in the deep basin hampers a correct understanding of the causes and consequences of OAE2.

Two recent model studies of ocean biogeochemistry during OAE2 suggest that extensive anoxia in the central deep basin of the proto-North Atlantic required low oxygen concentrations in the Pacific Ocean [*Monteiro et al*., 2012; *Ruvalcaba Baroni et al*., 2014]. This is because inflow of oxygen-rich waters from the Pacific would not have allowed for the development of full anoxia. Unfortunately, sediments capturing the OAE2 interval in the Pacific Ocean are scarce, and at present only a few continental margin sites have been studied [*Takashima et al*., 2011]. Validation of these model results therefore requires a data set that provides insight into the regional and temporal variability of redox conditions in the bottom waters of the deep basin of the proto-North Atlantic during OAE2.

Here we assess the spatial and temporal trends in bottom-water redox conditions during OAE2 in the deep proto-North Atlantic. For that purpose, we combine the existing geochemical data for DSDP Sites 367 and 603 with newly generated data for DSDP Site 386 and Ocean Drilling Program (ODP) Sites 641 and 1276 (Figure 1). Our redox proxies include ratios of C_{org}/P_{tot}, Fe/Al, and Mo/TOC and concentrations of various trace elements such as Mo and Mn. Our results highlight that water circulation in the proto-North Atlantic was severely restricted during OAE2. The deep part of the basin was fully anoxic for most of OAE2, except

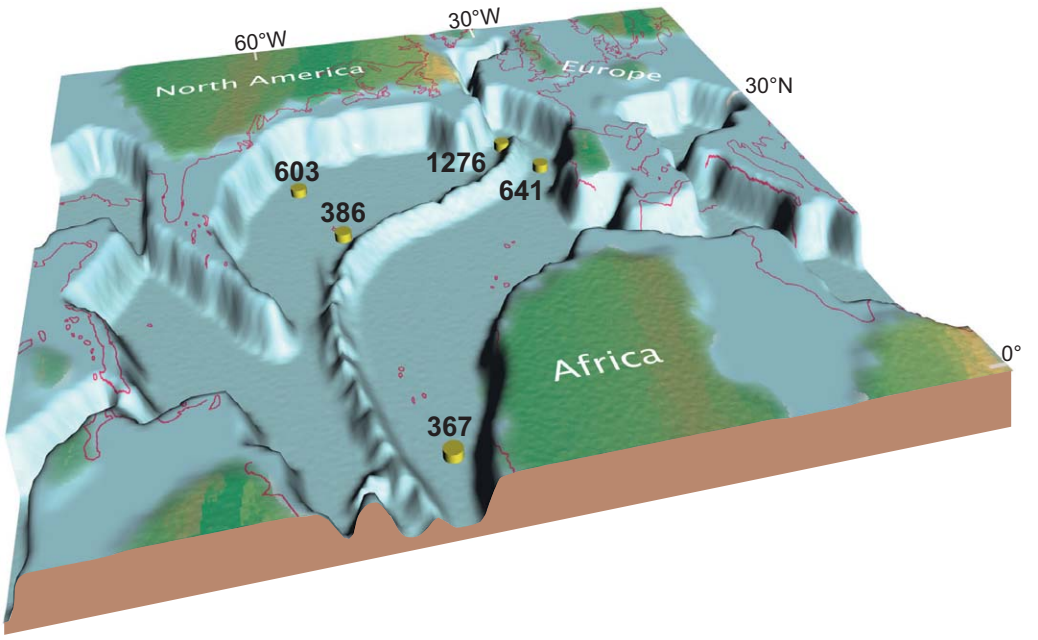

Figure 1. Three-dimensional paleogeographic map of the proto-North Atlantic basin for the Cenomanian Turonian boundary time interval, indicating the locations of the cores used in this study. Map adjusted from the map created at http://www.odsn.de/odsn/services/paleo-map/paleomap.html. Nonsubmerged landmasses in green are after *Scotese* [2001].

for what appears to have been a basin-wide oxygenation event within OAE2, associated with the "Plenus Cold Event" (PCE) [*Gale and Christensen*, 1996; *Forster et al*., 2007; *Sinninghe Damsté et al*., 2010].

2. Materials and Methods

2.1. Study Sites

All five sites in this study were located in the deep proto-North Atlantic during OAE2 (Figure 1). Estimated water depths, available from the literature (Table 1), range from 2000 to 4000 m and sediments over the CTBE-interval are pelagic or hemi-pelagic (Table 1). The sources of existing geochemical data for all DSDP and ODP sites and the newly generated data are listed in Table 2. Below, we describe the locations of the study sites and the lithology of the sediments covering the CTBE-interval.

2.1.1. Site 367: Cape Verde Basin, DSDP Leg 41

The southernmost site in this study is located offshore Senegal in the eastern equatorial Atlantic, on the abyssal plain in the vicinity of the mid-ocean ridge (12°29.2'N, 20°02.8'W, 4748 m water depth). A minor component of the CTBE sediments at Site 367 is composed of turbidities [*Shipboard Scientific Party*, 1977]. However, no direct evidence exists for a turbiditic origin for the OAE2-related black shales, which have been interpreted to reflect in situ pelagic sediments [*Kuypers et al*., 2002].

Table 1. Estimated Water Depth and Type of Sediment During OAE2

Site	Estimated Water Depth (m)	Type of Sediment
DSDP 367	3700[a]	Pelagic[b]
DSDP 386	2000–3800[a]	Pelagic[c]
DSDP 603	4000[a]	Hemipelagic[d]
ODP 641	3500[e]	Pelagic[e]
ODP 1276	>2000[f]	(Hemi)pelagic[f]

[a]*Chénet and Francheteau* [1979].
[b]*Shipboard Scientific Party* [1977].
[c]*Tucholke and Vogt* [1979].
[d]*Herbin et al*. [1987].
[e]*Shipboard Scientific Party* [1987b].
[f]*Urquhart et al*. [2007].

2.1.2. Site 386: Central Bermuda Rise, DSDP Leg 43

This site is the most centrally located site in this study, at ~140 km south-southeast of Bermuda (31°11.21'N, 64°14.94'W, 4793 m water depth). The CTBE sediments predominantly consist of multicolored, i.e., green, gray, and black, clay and mudstones that are interpreted as deep marine sediments [*Tucholke and Vogt*, 1979].

2.1.3. Site 603 (Hole B): Off Cape Hatteras, DSDP Leg 93

Site 603 was located in the northern part of the deep proto-North Atlantic. The site is located on the

Table 2. Overview of Data Sources and Original Publications

Site	Original Publication: Type of Data
DSDP 367	*Kuypers et al.* [2002]: $\delta^{13}C_{org}$, TOC, trace elements (ICP-AES) M. M. M. Kuypers (unpublished data, 2014): molar C_{org}/P_{tot} *Owens et al.* [2012]: Fe/Al
DSDP 386	This study
DSDP 603	*Herbin et al.* [1987]: TOC Selection of *Kuypers et al.* [2004a]: $\delta^{13}C_{org}$, TOC, trace elements (ICP-AES) *Kraal et al.* [2010]: molar C_{org}/P_{tot} *Owens et al.* [2012]: Fe/Al
ODP 641	This study
ODP 1276	*Sinninghe Damsté et al.* [2010]: $\delta^{13}C_{TOC}$, TOC This study: trace elements (ICP-OES)

western edge of the Hatteras Abyssal Plain, part of the North American Basin, 435 km west of Cape Hatteras (35°29.66'N, 70°01.70'W, 4644 m water depth) [*Shipboard Scientific Party*, 1987a]. The CTBE sediments consist of an alternation of organic-poor, often bioturbated green claystones, and organic-rich black shales [*Herbin et al.*, 1987]. Sedimentation at Site 603 was hemipelagic with some influence of coastal oceanic events [*Kuypers et al.*, 2004a].

2.1.4. Site 641 (Hole A): Galicia Bank, ODP Leg 103

The section at Site 641 was retrieved from the western margin of the Galicia Bank, offshore northwestern Spain (42°09.3'N, 12°10.9'W, 4646 m water depth). The Late Cenomanian-Early Turonian sediments consist of green and gray claystones. The OAE2 interval itself is represented by ~30 cm of dark green and black shales [*Shipboard Scientific Party*, 1987b].

2.1.5. Site 1276: Newfoundland Basin, ODP Leg 210

Site 1276, our most northerly site, is located in the Newfoundland Basin, offshore Canada (45°24.31980'N, 44°47.14960'W, 4565 m water depth). The mid-Cretaceous sequence predominantly consists of mud-dominated gravity flow deposits [*Shipboard Scientific Party*, 2004]. OAE2 itself is represented by a 3.5 m thick stack of mainly pelagic sediments [*Urquhart et al.*, 2007], concurrent with a drastic drop in the relative abundance of terrestrially derived palynomorphs (pollen and spores) [*Sinninghe Damsté et al.*, 2010].

2.2. Total Organic Carbon and Isotopes of Organic Carbon

Surfaces of selected sediment samples were scraped clean with a knife, freeze-dried and powdered and homogenized using a ceramic mortar and pestle. About 0.3 g of powdered sample was decalcified using 1M HCl. Subsequently sediment residues were analyzed for organic carbon content, from which TOC content was calculated after compensation for carbonate loss, and $\delta^{13}C_{TOC}$ (ts01, supporting information) using a Fisons Instruments CNS NA 1500 analyzer coupled to a Thermo Delta Plus isotope ratio spectrometer. Results were normalized to international standards. Average analytical uncertainty based on duplicate analyses of sediment samples was 0.01 wt. % for TOC and 0.02‰ for $\delta^{13}C_{TOC}$.

2.3. Major and Minor Element Compositions

Approximately 125 mg of freeze dried and powdered sample was dissolved in 2.5 mL mixed acid ($HClO_4$:HNO_3; 3:2) and 2.5 mL 40% HF, heated to 90°C and left overnight. The acids were evaporated at 160°C after which the residue was dissolved in 25 mL 4.5% HNO_3. Sediment elemental compositions were measured using Inductively Coupled Plasma-Optical Emission Spectrometry (ICP-OES; Perkin Elmer Optima 3000); the error calculated from standards and duplicates of the trace elements generally was <5% and never exceeded 15% for the elements used in this study, i.e., Mo, P, Fe, Al, Mn, Cr, V, Cu, Zn, Ni, and S (ts01, supporting information). Molybdenum values <20 ppm were below the background emission signal, and therefore have an error of >10%; these should, hence, be regarded as approximate values.

3. Results

3.1. Stratigraphy

At all five sites, the OAE2 interval was identified by chemostratigraphy based on an increase in TOC content combined with the characteristic CIE in C_{org} (Figure 2a). For Site 367, phases A and B of the CIE (isotopic "increase" and "plateau" phases, respectively) were identified based on a the CIE of ~6‰ in TOC, S-bound phytane [*Kuypers et al.*, 2002] and other biomarkers [*Sinninghe Damsté et al.*, 2008]. The "recovery," phase C, was not captured due to a coring gap. For DSDP Site 386, phase A of the OAE2 interval is absent due to a coring gap. A distinct 2.5‰ increase in $\delta^{13}C_{TOC}$ occurs right above the coring gap at 742.11 m below

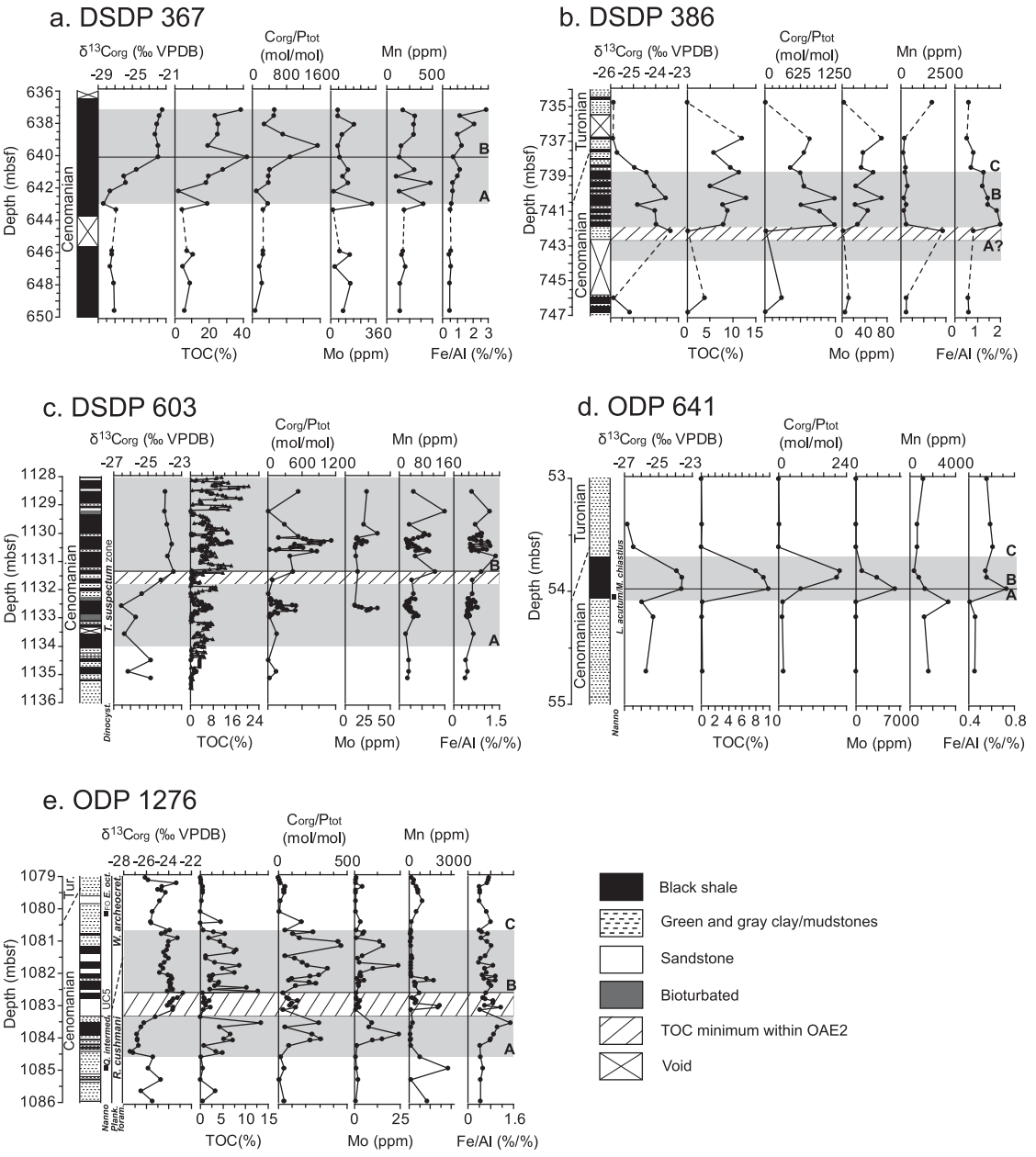

Figure 2. Lithology, chemostratigraphy ($\delta^{13}C_{org}/\delta^{13}C_{TOC}$ and TOC), C_{org}/P_{tot}, Mo, Mn, and Fe/Al for (a) Sites 367, (b) 386, (c) 603, (d) 641, and (e) 1276. Gray shades highlight the OAE2-interval, based on the positive excursion in $\delta^{13}C_{org}/\delta^{13}C_{TOC}$ and elevated TOC content, with the subdivision into different phases of the CIE marked by an "A," "B," or "C" after *Kuypers et al*. [2002]. Data sources are listed in Table 2. mbsf: meters below seafloor.

seafloor (mbsf) marking phase B of the event (Figure 2b). From 738.76 mbsf onward, isotopic values rapidly drop toward pre-OAE2 levels, indicating the start of phase C.

For DSDP Site 603, phases A and B were identified based on a ~2.5‰ positive CIE in TOC (Figure 2c) and a 4–5‰ positive shift in stable carbon isotopes of S-bound phytane [*Kuypers et al*., 2004a]. Similar to Site 367, phase C was not recovered at Site 603 due to a coring gap. Encountered dinocyst assemblages confirm a Cenomanian age for the studied sediments [*Habib and Drugg*, 1987] (Figure 2c).

Table 3. Average (Avg) and Maximum (Max) Values for TOC, TOC/Ptot, Mo, Mn, and Fe/Al, for Phases A and B of OAE2

		TOC (%)		C_{org}/P_{tot} (mol/mol)		Mo (ppm)		Mn (ppm)		Fe/Al (%/%)	
Site		Avg.	Max.	Avg.	Max.	Avg.	Max.	Avg.	Max.	Avg.	Max.
DSDP 367	Phase A	17	28	328	405	146	332	284	481	0.8	1.1
	Phase B	27	39	709	1536	86	185	230	308	1.5	2.9
DSDP 386	Phase A[a]										
	Phase B	8	13	778	1244	35	70	550	2320	1.4	2.0
DSDP 603	Phase A	3	11	173	501	21	36	45	126	0.6	0.9
	Phase B	7	19	539	1130	19	49	61	159	0.8	1.4
ODP 641	Phase A[b]										
	Phase B	9	10	167	216	3494	6206	824	1320	0.6	0.7
ODP 1276	Phase A	3	13	135	313	6	24	530	2161	0.8	1.5
	Phase B	5	13	198	457	6	24	322	1731	0.7	1.0

[a]At DSDP Site 386 phase A of OAE2 was not recovered/identified.
[b]Regarding the condensed nature of OAE2 at ODP Site 641, no values for phase A were derived.

For ODP Site 641 the OAE2 interval was previously identified based on stable carbon isotope stratigraphy [*Thurow et al*., 1988]. Here we determined a similar $\delta^{13}C_{TOC}$ profile, showing the isotopic "increase," phase A, from $-26.0‰$ at 54.10 mbsf to $-23.6‰$ at 53.98 mbsf, after a short plateau phase of ~20 cm, values drop back to the pre-excursion level (Figure 2d). Identification of the OAE2 interval at Site 641 was further confirmed by calcareous nannofossil biostratigraphy [*Shipboard Scientific Party*, 1987b]. The occurrence of *Lithraphidites acutum* and *Microstaurus chiastus* from ~54.1 to 54 mbsf (Figure 2d) are indicative for the Cenomanian-Turonian boundary [e.g., *Bralower et al*., 1997; *Luciani and Cobianchi*, 1999].

The OAE2-interval of ODP Site 1276 was identified based on a positive CIE of ~4.5‰ in TOC (Figure 2e) and a >5‰ in the stable isotopes of the bacterial biomarker C_{31} 17β,21β(H)-hopane [*Sinninghe Damsté et al*., 2010], and other biomarkers [*van Bentum et al*., 2012], clearly identifying all three phases of the CIE. Calcareous nannofossil and planktonic foraminifer biostratigraphy confirmed this age assignment [*Urquhart et al*., 2007] (Figure 2e).

3.2. TOC and C_{org}/P_{tot}

Site 367 exhibits the highest TOC concentrations during OAE2, with average values >15% and maximum values exceeding 30% (Figure 2a). For Sites 386, 603, 641, and 1276, TOC concentrations are elevated during OAE2, with average values ranging from 3 to 9% and maximum values between 10 and 19% (Figure 2 and Table 3). Downcore variations in the TOC profile is high, particularly for Sites 603 and 1276. Intriguingly, the TOC profiles for Sites 386, 603, and 1276 show a distinct minimum within OAE2, with TOC <1%, close to the transition from the A phase to the B phase of the CIE (Figure 2).

At all five sites, C_{org}/P_{tot} ratios are high (above the Redfield ratio of 106 associated with organic matter production) during OAE2 (Figure 2). Average and maximum values are, however, much higher for the three most western Sites 367, 386, and 603. Average values for phase B range from 500 to 800 with maxima up to ~1500, compared to values of around 200 (maxima up to ~450) for Sites 641 and 1276 (Figure 2 and Table 3). Again, a minimum in C_{org}/P_{tot} ratios is observed within OAE2 for Sites 386, 603, and 1276, at the same stratigraphic interval as the TOC minimum mentioned above.

3.3. Trace Elements and Trace Elemental Ratios

Concentrations of the trace metals Mo (Figure 2 and Table 3), V, Cr, Ni, Zn, and Cu (Figure fs01, supporting information) generally increase within the OAE2 interval for Sites 386, 603, and 1276, although downcore variability ranges up to one order of magnitude for some trace metals, particularly for the latter two sites. For Site 367, no distinct increase in the concentration of trace metals was recorded across the transition to OAE2, except for Ni concentrations, which more than double. In terms of absolute values, there is great diversity between sites and all trace elements. Extreme enrichments in trace metals are observed (e.g., up to 6000 ppm for Mo) in the condensed OAE2 section at Site 641 (Figures 2 and fs01, supporting information). In contrast with the elements listed above, Mn decreases within the OAE2 or remains low (Sites 367 and 603).

3.3.1. Fe/Al Ratios

Ratios of Fe/Al are near the crustal average of ~0.5 [*Taylor and McLennan*, 1995] at all sites prior to and after OAE2 (Figure 2 and Table 3). During the event, values are typically >1 for Sites 367 and 386, with maximum

values around 2.9 and 2.0, respectively. At Sites 603 and 1276 pre-event average Fe/Al values of ~0.7 increase to maximum values close to 1.5 during the CIE, indicating a modest increase. At Site 641 only one data point shows a distinct increase relative to background crustal values, with a value of 0.7 (Figure 2 and Table 3). For all sites the S contents follow the trends in Fe/Al ratios (Figure fs01, supporting information).

3.3.2. Mo/TOC Ratios

Ratios of Mo/TOC (ts01, supporting information) for the OAE2 interval of Sites 367 and 386 are quite similar, and generally range between 3 and 5. Average Mo/TOC ratios for Sites 603 and 1276 are lower at ~3 and ~2, respectively. Site 641 shows values >100, resulting from the unusually high Mo concentrations measured at this site.

4. Discussion

4.1. Distribution and Degree of Oxygen Depletion

The southern part of the proto-North Atlantic, which was located in the equatorial zone during the Late Cretaceous, was highly productive prior to and during OAE2, based on bulk geochemical data and calcareous nannofossil assemblages [e.g., *Kuypers et al*., 2002; *Hardas and Mutterlose*, 2007]. Furthermore, multiple studies provide evidence for euxinia extending into the photic zone, based on high concentrations of the biomarkers isorenieratane, chlorobactane, and maleimide, molecular remains of the brown strain of green sulfur bacteria, that require both light and free sulfide [*Sinninghe Damsté and Köster*, 1998; *Kuypers et al*., 2002; *Pancost et al*., 2004; *van Bentum et al*., 2009]. The high TOC and C_{org}/P_{tot} contents for Site 367 are the result of high export productivity and anoxic conditions, as P is regenerated from the sediments under anoxic conditions [*Ingall et al*., 1993; *Ingall and Jahnke*, 1994], resulting in an elevated C_{org}/P_{tot} ratio. Low Mn concentrations, elevated Mo and increasing Fe/Al confirm the reducing conditions in the bottom waters at this site and in the surrounding area (Figure 2a and Table 3). However, the maximum concentrations for Mo, V, Zn, Cr, and Cu are observed prior to OAE2 (Figures 2a and fs01, supporting information). This was previously documented for ODP Sites 1258 and 1260, which are also located in the southern part of the proto-North Atlantic [*Hetzel et al*., 2009] and was attributed to a shift from regional, southern proto-North Atlantic anoxia, to basin-scale anoxia, ultimately leading to a drawdown of the seawater trace-metal reservoir [*Hetzel et al*., 2009]. The combined existing and newly generated data for our sites, distributed throughout the proto-North Atlantic, highlight the temporal and spatial variability in redox conditions in the deep basin of the proto-North Atlantic during OAE2.

At Site 386, in the central part of the proto-North Atlantic, high TOC values and extremely high C_{org}/P_{tot} values in combination with elevated trace-metal concentrations and a minimum in Mn concentrations, indicate that bottom waters were anoxic and sulfidic during OAE2 (Figures 2b and fs01, supporting information). Sediment Fe/Al ratios increased across the OAE2 interval, suggesting an expanding oxygen-depleted zone. In phase C of the CIE, TOC, C_{org}/P_{tot}, and trace-metal concentrations remained high, suggesting that anoxia persisted at this site in the central part of the proto-North Atlantic. During this phase, Fe/Al ratios declined, however, indicating either a smaller oxygen-depleted zone or more sulfidic conditions [*Scholz et al*., 2014]. Although anoxia seems to have continued locally after OAE2 at Site 386, the decline of the Fe/Al ratio most likely reflects a reduction in oxygen depletion in the surrounding area.

The northerly Sites 603 and 1276, both show very distinctive TOC, C_{org}/P_{tot}, and trace-metal enrichments for the OAE2 interval (Figures 2c, 2e, and fs01, supporting information). In comparison to Sites 367, 386, and 641, average concentrations (Table 3) remained relatively low, however, with exception of the Mn concentrations at Site 1276. We interpret this to reflect comparatively less severe oxygen depletion in the northern part of the deep proto-North Atlantic basin. The repeated fluctuations in TOC with values that are frequently close to zero, and variations in lithology, i.e., variations between laminated organic-rich black shales and organic-poor sand, clay, and mudstones (Figures 2c and 2e), i.e., even suggest temporary oxygenation. For both sites the presence of the biomarker for photic-zone euxinia, isorenieratane, has been demonstrated [*Kuypers et al*., 2004a; *van Bentum et al*., 2012]. Isorenieratane was, however, only present in very low quantities and only in the most organic-rich parts of the section. This supports sporadic occurrences of photic-zone euxinia at these sites, but excludes persistent photic-zone euxinia as reported for the southern, equatorial part of the proto-North Atlantic [*Sinninghe Damsté and Köster*, 1998; *Kuypers et al*., 2002; *van Bentum et al*., 2009]. For both sites, Mn concentrations are low during OAE2, supporting anoxic conditions at the

sediment-water interface. At the same time Fe/Al is elevated, suggesting expansion of the area with oxygen-depleted bottom waters in the surrounding part of the basin.

Site 641 clearly had anoxic bottom waters during OAE2, reflected in the distinct black shale layer with a TOC content of ~10%. Isorenieratane was reported [*Sinninghe Damsté and Köster*, 1998], but again in low quantities. Trace-metal enrichments are, however, extreme, e.g., Mo concentrations up to 6000 ppm [*Thurow et al*., 1988, and this study] (Figures 2d and fs01, supporting information). Such extreme enrichments might result from proximity to the mid-ocean ridge. The mid-ocean ridge was very active during the mid-Cretaceous [e.g., *Hays and Pitman*, 1973; *Larson*, 1991; *Cogné and Humler*, 2004], and associated vent systems most likely introduced large amounts of trace metals into bottom waters [e.g., *Douville et al*., 2002]. During periods of anoxia, these trace metals would be scavenged from the water column directly, resulting in the observed extreme enrichments in the sediment. However, ratios of Fe/Al do not show a large increase at Site 641, conflicting with this hydrothermal input scenario [e.g., *Owens et al*., 2012]. Furthermore, Sites 386 and 1276 are also positioned close to the mid-ocean ridge and do not show such extreme enrichments.

The most straightforward explanation for the extreme trace-metal concentrations is that they did not result from high fluxes but rather from very low sedimentation rates at Site 641. A similar relationship between low sedimentation rates and high authigenic trace-metal concentrations was inferred for Pennsylvanian black shales [*Algeo and Maynard*, 2004; *Algeo and Heckel*, 2008]. Average sedimentation rates during OAE2 at Site 641 would have been in the order of 0.25 cm kyr^{-1}, when assuming a constant rate of sedimentation, 80% compaction of clays after deposition [*Hedberg*, 1936] and a ~600 kyr long duration for the positive CIE [e.g., *Meyers et al*., 2012]. These sedimentation rates are common for seamounts [*Kukal*, 1990]. It is unclear, however, whether Site 641 was located on such a height. Periods of typical pelagic sedimentation at rates of 2–4 cm kyr^{-1} [*Kukal*, 1990] may also have alternated with periods without net sediment deposition.

The supply of trace metals at the site could have been augmented by input from relatively oxic water masses, for example, originating from the intermittent (sub)oxic northern Tethyan realm [e.g., *Westermann et al*., 2010; *Hetzel et al*., 2011]. Unfortunately our knowledge of mid-Cretaceous ocean and bottom water currents is not sufficient to prove or disprove the latter suggestion.

Our results suggest that the entire deep proto-North Atlantic basin was anoxic during a major part of OAE2. Based on our paleoredox proxies, we conclude that there were large spatial differences in the degree of oxygen depletion during the event (Figure 3). Anoxia and euxinia were particularly severe in the southern part of the basin, where bottom waters were already euxinic before OAE2 (Figure 3), in perfect agreement with the isorenieratene derivatives and other biomarker proxies [*Sinninghe Damsté et al*., 2014]. In contrast, the bottom waters of the northern part of the deep proto-North Atlantic were not anoxic prior to and after OAE2, and were intermittently anoxic during a major part of the event (Figure 3). Bottom waters in the central, deep basin were likely anoxic and sulfidic throughout the event, but may have been overlain by oxic/suboxic intermediate waters [*Ruvalcaba Baroni et al*., 2014]. Crucially, according to modeling experiments, the inflow of low-oxygen waters from the Pacific Ocean is required to have maintained widespread anoxia in the central, deep proto-North Atlantic basin throughout OAE2 [*Monteiro et al*., 2012; *Ruvalcaba Baroni et al*., 2014].

4.2. Water Mass Renewal Rates

Under euxinic conditions molybdate anions are converted to particle-reactive thiomolybdates, hence allowing for burial of Mo in the sediments [*Helz et al*., 1996]. As a result of this more rapid burial of Mo, it was shown for modern euxinic basins that the renewal time of the deep water mass, which is a function of multiple factors ranging from tectonic restriction of a basin to the rates of overturning, mixing, and circulation in a basin, can be estimated from the regression slope of Mo with TOC [*Algeo and Lyons*, 2006]. This proxy was successfully applied to Mesozoic sediments [*McArthur et al*., 2008; *Westermann et al*., 2013]. For the Early Toarcian OAE, the degree of water mass restriction was shown to be strongest at greater water depth [*McArthur et al*., 2008]. Very low Mo/TOC ratios in sediments deposited during OAE2 in the Tethys Ocean have been suggested to reflect extreme restriction of the water mass, i.e., a long renewal period of deep water [*Westermann et al*., 2013]. Low Mo/TOC ratios for the equatorial sites at Demarara Rise (ODP Sites 1258 and 1260) during OAE2 have also been attributed to a restricted circulation [*Hetzel et al*., 2009; *Algeo and Rowe*, 2012].

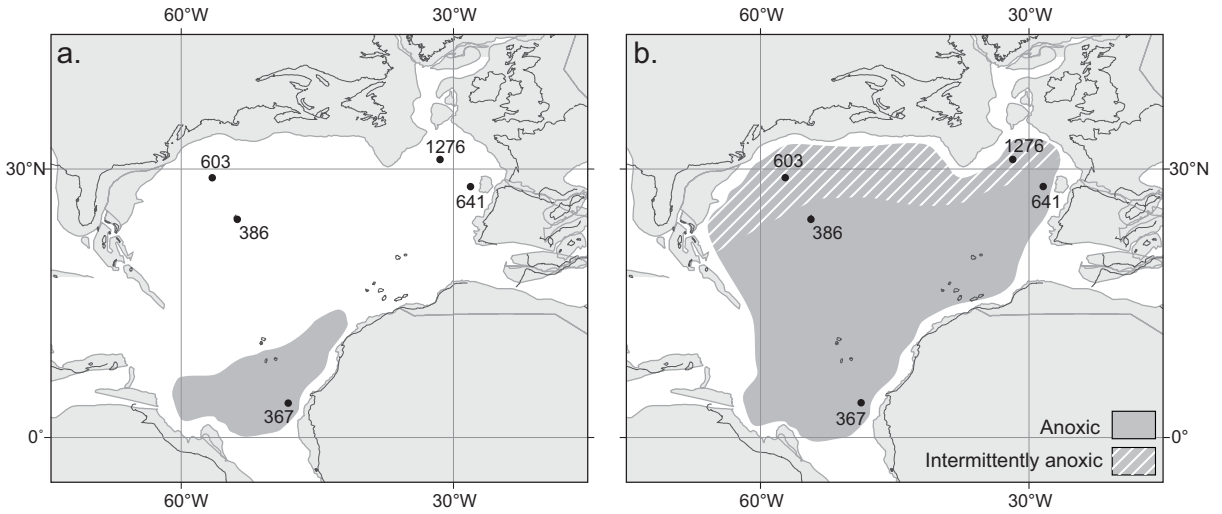

Figure 3. Schematic, showing the progressive change in oxygenation of bottom waters across the basin from (a) the situation prior to OAE2 to (b) the situation during OAE2. Maps were created at http://www.odsn.de/odsn/services/paleomap/paleomap.html.

At present, the Black Sea is the marine euxinic basin with the longest deep water renewal time, due to its tectonic restriction and lack of vertical mixing. This is reflected by ratios of Mo/TOC for Black Sea sediments, which plot at a regression slope of 4.5 ± 1 (Figure 4), corresponding to a renewal period for Black Sea deep water in the range of 500–4000 years. For comparison, the regression slope for Saanich Inlet, which is a modern, relatively shallow, euxinic basin with only minor tectonic restriction, is 45 ± 5 (Figure 4), corresponding to a renewal period of deep water of only ~1.5 years [*Algeo and Lyons*, 2006, and references therein] (Figure 4).

The Mo/TOC data for sediments deposited under anoxic bottom waters during the OAE2 interval, as compiled in this study, can be used to quantify the degree of restriction for proto-North Atlantic deep water. The Mo/TOC data for Site 641 were excluded, because the extremely enriched values seem to be the result of the condensed OAE2 interval. Mo/TOC data for the four remaining Sites 367, 386, 641, and 1276 are within the same range. The Mo/TOC data are characterized by a regression slope of ~4.1 with a R^2 of 0.43 (Figure 4).

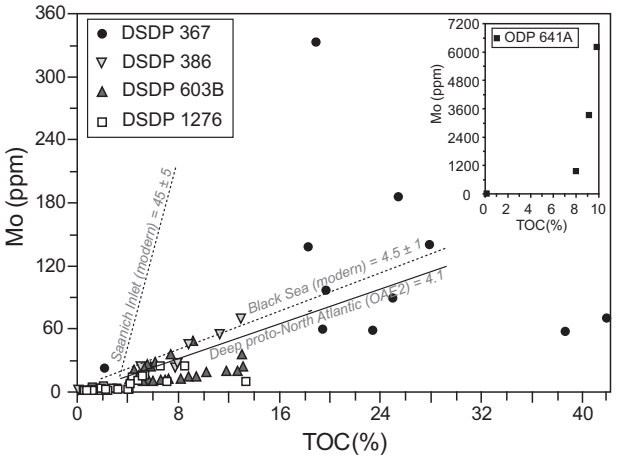

Figure 4. Crossplot of sediment Mo versus TOC for the OAE2-interval at the studied sites. Dashed lines show regression slopes for Mo and TOC data of two modern anoxic marine environments, the minor restricted Saanich Inlet and the severely restricted Black Sea [*Algeo and Lyons*, 2006]. The solid line is the combined regression slope of the four (DSDP 367, DSDP 386, DSDP 603, and ODP 1276) deep proto-North Atlantic sites during OAE2.

The regression slope for Mo/TOC data of the OAE2 interval in the proto-North Atlantic thus almost equals the regression slope for Mo/TOC in the modern Black Sea, which suggests a similar renewal period for proto-North Atlantic deep water during OAE2, i.e., 500–4000 years. This renewal period is relatively short compared with the renewal period that could be calculated for the OAE2-interval at Demerara Rise ODP Sites 1258 and 1260 (Mo/TOC of 2–3) [*Hetzel et al.*, 2009] or the renewal period for the stagnant, i.e., very poor vertical mixing of the water column,

Cleveland Basin during the Toarcian-OAE (Mo/TOC of ~0.5) [*McArthur et al*., 2008]. The renewal period for deep waters in the proto-North Atlantic during OAE2 is, however, still considerably longer when compared with the ~200 year period for the present-day northern Atlantic [*Broecker*, 1991].

Although the renewal period for deep waters during OAE2 was much longer then at present, we infer that deep waters in the proto-North Atlantic basin were far from stagnant, in line with results from modeling studies [e.g., *Monteiro et al*., 2012; *Ruvalcaba Baroni et al*., 2014].

4.3. A Basinwide Oxygenation Event?

At Site 1276 the organic-rich deposits of OAE2 are interrupted by an organic-poor interval with a thickness of ca. 75 cm, between 1082.39 and 1083.13 mbsf (Figure 2e). Along with low TOC concentrations (<2.3 wt. %) [*Sinninghe Damsté et al*., 2010], this interval is also characterized by low trace-metal concentrations (Figure 2e). Both suggest that conditions at the sediment-water interface were less reducing during this period. Mean annual average sea-surface temperature reconstructions, using TEX_{86} paleothermometry, show a concomitant 5–11°C cooling, attributed to a drop in atmospheric CO_2 resulting from the widespread burial of organic matter [*Sinninghe Damsté et al*., 2010]. This cooling is synchronous with an incursion of boreal fauna in the shelf seas of NW Europe and was called the "Plenus Cold Event" (PCE) [*Jefferies*, 1962; *Gale and Christensen*, 1996]. The PCE-related cooling has now been recognized throughout the proto-North Atlantic in different paleoenvironmental settings, i.e., in the deep basin (DSDP Site 367) [*Forster et al*., 2007], in intermediate waters (ODP Site 1260) [*Forster et al*., 2007], and in shallow-marine environments [e.g., *van Helmond et al*., 2014], and coincident with minima in TOC and trace-metal concentrations at several sites, although not at Site 367.

The lowest data point within the recovered OAE2 interval at Site 386 shows that anoxia might not have persisted throughout the entire event at this site either, as concentrations of TOC, Mo, and other trace elements are close to zero and the Mn content increases. This is indicative of less reducing or even oxic conditions at the seafloor. Unfortunately the OAE2 interval at Site 386 is not complete and the stratigraphy lacks detail; therefore, it is impossible to confirm whether this data point represents the PCE. At Site 603, the OAE2 interval also contains a section with low TOC values between 1131.85 and 1131.4 mbsf. Although C_{org}/P, Mo, and other trace elements are low for this interval, similar values are recorded for organic-rich parts of the OAE2 interval. The stratigraphic position of the interval with TOC values at Site 603 relative to the CIE does, however, does match the organic-lean interval at Site 1276, where it was linked with the PCE. Therefore, we consider it likely that this interval also represents the PCE at Site 603.

Based on our findings, we suggest that the PCE led to substantial, temporary re-oxygenation of bottom waters during OAE2, throughout the proto-North Atlantic, including the deep basin.

5. Conclusions

Newly generated and compiled existing redox proxy data for five deep-sea sites distributed over the proto-North Atlantic confirm that the entire deep proto-North Atlantic was anoxic during most of OAE2. Based on our data, however, spatial differences in redox conditions existed within the basin, with persistent severe anoxia and euxinia in the southern proto-North Atlantic, and only intermittently anoxic bottom waters in the northern proto-North Atlantic.

The regression slope of the Mo and TOC data for the OAE2 interval for the presented sites is similar to that of the modern euxinic Black Sea. This suggests that circulation in the proto-North Atlantic basin was severely restricted during OAE2.

Finally, a previously identified oxygenation event within OAE2, associated with the Plenus Cold Event, has been found in the sediments of multiple deep-sea sites as well. This implies that during this event, bottom water oxygenation not only occurred on the shelves and in epicontinental seas but also in the deep sea.

Acknowledgments

All data used and discussed in the current paper are listed and depicted in the supporting information ts01 and fs01. We thank T. Algeo and an anonymous reviewer for their constructive comments and suggestions. This research was supported by the "Focus & Massa project" of Utrecht University granted to H. Brinkhuis and C. P. Slomp and additional financial support by Statoil. The European Research Council under the European Community's Seventh Framework Program provided funding for this work by ERC Starting grant 278364 to C. P. Slomp and 259627 to A. Sluijs. This research used samples provided by the Integrated Ocean Drilling Program (IODP). Marcel M. M. Kuypers is kindly thanked for sharing unpublished data of DSDP Site 367. Arnold van Dijk and Ton Zalm are thanked for analytical assistance and Ton Markus for illustration support.

References

Algeo, T. J., and P. H. Heckel (2008), The Late Pennsylvanian midcontinent sea of North America: A review, *Palaeogeogr. Palaeoclimatol. Palaeoecol.*, *268*, 205–221, doi:10.1016/j.palaeo.2008.03.049.

Algeo, T. J., and E. Ingall (2007), Sedimentary Corg:P ratios, paleocean ventilation, and Phanerozoic atmospheric pO_2, *Palaeogeogr. Palaeoclimatol. Palaeoecol.*, *256*, 130–155, doi:10.1016/j.palaeo.2007.02.029.

Algeo, T. J., and T. W. Lyons (2006), Mo-total organic carbon covariation in modern anoxic marine environments: Implications for analysis of paleoredox and paleohydrographic conditions, *Paleoceanography*, *21*, PA1016, doi:10.1029/2004PA001112.
Algeo, T. J., and J. B. Maynard (2004), Trace-element behavior and redox facies in core shales of Upper Pennsylvanian Kansas-type cyclothems, *Chem. Geol.*, *206*, 289–318, doi:10.1016/j.chemgeo.2003.12.009.
Algeo, T. J., and H. Rowe (2012), Paleoceanographic applications of trace-metal concentration data, *Chem. Geol.*, *324–325*, 6–18, doi:10.1016/j.chemgeo.2011.09.002.
Arthur, M. A., and B. B. Sageman (1994), Marine black shales: Depositional mechanisms and environments of ancient deposits, *Annu. Rev. Earth Planet. Sci.*, *22*, 499–551, doi:10.1146/annurev.ea.22.050194.002435.
Arthur, M. A., W. E. Dean, and L. M. Pratt (1988), Geochemical and climatic effects of increased marine organic-carbon burial at the Cenomanian Turonian boundary, *Nature*, *335*, 714–717, doi:10.1038/335714a0.
Barclay, R. S., J. C. McElwain, and B. B. Sageman (2010), Carbon sequestration activated by a volcanic CO_2 pulse during Ocean Anoxic Event 2, *Nat. Geosci.*, *3*, 205–208, doi:10.1038/ngeo757.
Bice, K. L., D. Birgel, P. A. Meyers, K. A. Dahl, K.-U. Hinrichs, and R. D. Norris (2006), A multiple proxy and model study of the Cretaceous upper ocean temperatures and atmospheric CO_2 concentrations, *Paleoceanography*, *21*, PA2002, doi:10.1029/2005PA001203.
Bralower, T. J., P. D. Fullagar, C. K. Paull, G. S. Dwyer, and R. M. Leckie (1997), Mid-Cretaceous strontium-isotope stratigraphy of deep-sea sections, *Geol. Soc. Am. Bull.*, *109*, 1421–1442, doi:10.1130/0016-7606(1997)109<1421:MCSISO>2.3.CO.
Broecker, W. S. (1991), The great ocean conveyor, *Oceanography*, *4*, 79–89.
Brumsack, H. J. (1980), Geochemistry of Cretaceous black shales from the Atlantic Ocean (DSDP Legs 11, 14, 36 and 41), *Chem. Geol.*, *31*, 1–25, doi:10.1016/0009-2541(80)90064-9.
Canfield, D. E., T. W. Lyons, and R. Raiswell (1996), A model for iron deposition to euxinic Black Sea sediments, *Am. J. Sci.*, *296*, 818–834.
Chénet, P. Y., and J. Francheteau (1979), Bathymetric reconstruction method: Application to the Central Atlantic Basin between 10°N and 40°N, in *Deep Sea Drilling Project Initial Report, 51, 52, 53, Part 2*, pp. 1501–1514, U.S. Gov. Print. Off., Washington, D. C.
Cogné, J. P., and E. Humler (2004), Temporal variation of oceanic spreading and crustal production rates during the last 180 My, *Earth Planet. Sci. Lett.*, *227*, 427–439, doi:10.1016/j.epsl.2004.09.002.
Douville, E., J. L. Charlou, E. H. Oelkers, P. Bienvenu, C. F. J. Colon, J. P. Donval, Y. Fouquet, D. Prieur, and P. Appriou (2002), The rainbow vent fluids (36°14′N, MAR): The influence of ultramafic rocks and phase separation on trace metal content in Mid-Atlantic Ridge hydrothermal fluids, *Chem. Geol.*, *184*, 37–48, doi:10.1016/S0009-2541(01)00351-5.
Eckert, S., H.-J. Brümsack, S. Severmann, B. Schnetger, C. März, and H. Fröllje (2013), Establishment of euxinic conditions in the Holocene Black Sea, *Geology*, *41*, 431–434, doi:10.1130/G33826.1.
Emerson, S. R., and S. S. Huested (1991), Ocean anoxia and the concentrations of molybdenum and vanadium in seawater, *Mar. Chem.*, *34*(3), 177–196, doi:10.1016/0304-4203(91)90002-E.
Forster, A., S. Schouten, K. Moriya, P. A. Wilson, and J. S. Sinninghe Damsté (2007), Tropical warming and intermittent cooling during the Cenomanian/Turonian Oceanic Anoxic Event (OAE 2): Sea surface temperature records from the equatorial Atlantic, *Paleoceanography*, *22*, PA1219, doi:10.1029/2006PA001349.
Gale, A. S., and W. K. Christensen (1996), Occurrence of the belemnite Actinocamax plenus in the Cenomanian of SE France and its significance, *Bull. Geol. Soc. Den.*, *43*, 68–77.
Habib, D., and W. S. Drugg (1987), Palynology of Sites 603 and 605, Leg 93, in *Deep Sea Drilling Project Initial Report*, edited by J. E. van Hinte et al., vol. 93, pp. 751–775, U.S. Gov. Print. Off., Washington, D. C.
Hardas, P., and J. Mutterlose (2007), Calcareous nannofossil assemblages of Oceanic Anoxic Event 2 in the equatorial Atlantic: Evidence of an eutrophication event, *Mar. Micropaleontol.*, *66*, 52–69, doi:10.1016/j.marmicro.2007.07.007.
Hays, J. D., and W. C. Pitman III (1973), Lithospheric plate motion, sea level changes and climatic and ecological consequences, *Nature*, *246*, 18–22.
Hedberg, H. D. (1936), Gravitational compaction of clays and shales, *Am. J. Sci.*, *184*, 241–287.
Helz, G. R., C. V. Miller, J. M. Charnock, J. F. W. Mosselmans, R. A. D. Pattrick, C. D. Garner, and D. J. Vaughan (1996), Mechanism of molybdenum removal from the sea and its concentration in black shales: EXAFS evidence, *Geochim. Cosmochim. Acta*, *60*, 3631–3642, doi:10.1016/0016-7037(96)00195-0.
Herbin, J. P., E. Masure, and J. Roucaché (1987), Cretaceous formations from the lower continental rise off Cape Hatteras: Organic geochemistry, dinoflagellate cysts, and the Cenomanian/Turonian boundary event at Sites 603 (Leg 93) and 105 (Leg 11), in *Deep Sea Drilling Project Initial Report*, vol. 93, pp. 1139–1160, U.S. Gov. Print. Off., Washington, D. C.
Hetzel, A., M. E. Böttcher, U. G. Wortmann, and H.-J. Brumsack (2009), Paleo-redox conditions during OAE 2 reflected in Demerara Rise sediment geochemistry (ODP Leg 207), *Palaeogeogr. Palaeoclimatol. Palaeoecol.*, *273*, 302–328, doi:10.1016/j.palaeo.2008.11.005.
Hetzel, A., C. März, C. Vogt, and H.-J. Brumsack (2011), Geochemical environment of Cenomanian–Turonian black shale deposition at Wunstorf (northern Germany), *Cretaceous Res.*, *32*, 480–494, doi:10.1016/j.cretres.2011.03.004.
Higgins, M. B., R. S. Robinson, J. M. Husson, S. J. Carter, and A. Pearson (2012), Dominant eukaryotic export production during ocean anoxic events reflects the importance of recycled NH_4^+, *Proc. Natl. Acad. Sci. U. S. A.*, *109*, 2269–2274, doi:10.1073/pnas.1104313109.
Ingall, E., and R. Jahnke (1994), Evidence for enhanced phosphorus regeneration from marine sediments overlain by oxygen depleted waters, *Geochim. Cosmochim. Acta*, *58*, 2571–2575, doi:10.1016/0016-7037(94)90033-7.
Ingall, E. D., R. M. Bustin, and P. Van Cappellen (1993), Influence of water column anoxia on the burial and preservation of carbon and phosphorus in marine shales, *Geochim. Cosmochim. Acta*, *57*, 303–316, doi:10.1016/0016-7037(93)90433-W.
Jefferies, R. P. S. (1962), The palaeoecology of the *Actinocamax plenus* subzone (lowest Turonian) in the Anglo-Paris Basin, *Palaeontology*, *4*, 609–647.
Kraal, P., C. P. Slomp, A. Forster, and M. M. M. Kuypers (2010), Phosphorus cycling from the margin to abyssal depths in the proto-Atlantic during oceanic anoxic event 2, *Palaeogeogr. Palaeoclimatol. Palaeoecol.*, *295*, 42–54, doi:10.1016/j.palaeo.2010.05.014.
Kukal, Z. (1990), The rate of geological processes, *Earth Sci. Rev.*, *28*, 7–258.
Kuroda, J., N. O. Ogawa, M. Tanimizu, M. F. Coffin, H. Tokuyama, H. Kitazato, and N. Ohkouchi (2007), Contemporaneous massive subaerial volcanism and Late Cretaceous oceanic anoxic event 2, *Earth Planet. Sci. Lett.*, *256*, 211–223, doi:10.1016/j.epsl.2007.01.027.
Kuypers, M. M. M., R. D. Pancost, I. A. Nijenhuis, and J. S. Sinninghe Damsté (2002), Enhanced productivity led to increased organic carbon burial in the euxinic North Atlantic basin during the late Cenomanian oceanic anoxic event, *Paleoceanography*, *17*, PA1052, doi:10.1029/2000PA000569.
Kuypers, M. M. M., L. J. Lourens, W. R. C. Rijpstra, R. D. Pancost, I. A. Nijenhuis, and J. S. Sinninghe Damsté (2004a), Orbital forcing of organic carbon burial in the proto-North Atlantic during oceanic anoxic event 2, *Earth Planet. Sci. Lett.*, *228*, 465–482, doi:10.1016/j.epsl.2004.09.037.
Kuypers, M. M. M., Y. van Breugel, S. Schouten, E. Erba, and J. S. Sinninghe Damsté (2004b), N_2-fixing cyanobacteria supplied nutrient N for Cretaceous oceanic anoxic events, *Geology*, *32*, 853–856, doi:10.1130/G20458.1.

Larson, R. L. (1991), Latest pulse of Earth: Evidence for a mid-Cretaceous superplume, *Geology*, *19*, 547–550, doi:10.1130/00917613(1991)019<0547:LPOEEF>2.3.CO;2.
Leckie, R. M., T. J. Bralower, and R. Cashman (2002), Oceanic anoxic events and plankton evolution: Biotic response to tectonic forcing during the mid-Cretaceous, *Paleoceanography*, *17*(3), 1041, doi:10.1029/2001PA000623.
Lenz, C., T. Behrends, T. Jilbert, M. Silveira, and C. P. Slomp (2014), Redox-dependent changes in manganese speciation in Baltic Sea sediments from the Holocene Thermal Maximum: An EXAFS, XANES and LA-ICP-MS study, *Chem. Geol.*, *370*, 49–57, doi:10.1016/j.chemgeo.2014.01.013.
Luciani, V., and M. Cobianchi (1999), The Bonarelli Level and other black shales in the Cenomanian-Turonian of the northeastern Dolomites (Italy): Calcareous nannofossil and foraminiferal data, *Cretaceous Res.*, *20*, 135–167, doi:10.1006/cres.1999.0146.
Lyons, T. W., and S. Severmann (2006), A critical look at iron paleoredox proxies: New insights from modern euxinic marine basins, *Geochim. Cosmochim. Acta*, *70*, 5698–5722, doi:10.1016/j.gca.2006.08.021.
McArthur, J. M., T. J. Algeo, B. van de Schootbrugge, Q. Li, and R. J. Howarth (2008), Basinal restriction, black shales, Re–Os dating, and the early Toarcian (Jurassic) oceanic anoxic event, *Paleoceanography*, *23*, PA4217, doi:10.1029/2008PA001607.
Meyers, S. R., B. B. Sageman, and M. A. Arthur (2012), Obliquity forcing and the amplification of high-latitude climate processes during Oceanic Anoxic Event 2, *Paleooceanography*, *27*, PA3212, doi:10.1029/2012PA002286.
Monteiro, F. M., R. D. Pancost, A. Ridgwell, and Y. Donnadieu (2012), Nutrients as the dominant control on the spread of anoxia and euxinia across the Cenomanian–Turonian oceanic anoxic event (OAE2): Model–data comparison, *Paleoceanography*, *27*, PA4209, doi:10.1029/2012PA002351.
Morel, F. M. M., and N. M. Price (2003), The biogeochemical cycles of trace metals in the oceans, *Science*, *300*, 944–947, doi:10.1126/science.1083545.
Mort, H. P., T. Adatte, K. B. Föllmi, G. Keller, P. Steinmann, V. Matera, Z. Berner, and D. Stuben (2007), Phosphorus and the roles of productivity and nutrient recycling during oceanic anoxic event 2, *Geology*, *35*, 483–486, doi:10.1130/G23475A.1.
Owens, J. D., T. W. Lyons, X. Li, K. G. Macleod, G. Gordon, M. M. M. Kuypers, A. Anbar, W. Kuhnt, and S. Severmann (2012), Iron isotope and trace metal records of iron cycling in the proto-North Atlantic during the Cenomanian–Turonian oceanic anoxic event (OAE-2), *Paleoceanography*, *27*, PA3223, doi:10.1029/2012PA002328.
Pancost, R. D., N. Crawford, S. Magness, A. Turner, H. C. Jenkyns, and J. R. Maxwell (2004), Further evidence for the development of photic-zone euxinic conditions during Mesozoic oceanic anoxic events, *J. Geol. Soc. London*, *161*(3), 353–364, doi:10.1144/0016764903-059.
Pogge von Strandmann, P. A. E., H. C. Jenkyns, and R. G. Woodfine (2013), Lithium isotope evidence for enhanced weathering during Oceanic Anoxic Event 2, *Nat. Geosci.*, *6*, 668–672, doi:10.1038/ngeo1875.
Reed, D. C., C. P. Slomp, and G. J. de Lange (2011), A quantitative reconstruction of organic matter and nutrient diagenesis in Mediterranean Sea sediments over the Holocene, *Geochim. Cosmochim. Acta*, *75*, 5540–5558, doi:10.1016/j.gca.2011.07.002.
Ruvalcaba Baroni, I., R. P. M. Topper, N. A. G. M. van Helmond, H. Brinkhuis, and C. P. Slomp (2014), Biogeochemistry of the North Atlantic during oceanic anoxic event 2: Role of changes in ocean circulation and phosphorus input, *Biogeosciences*, *11*, 977–993, doi:10.5194/bg-11-977-2014.
Schlanger, S. O., and H. C. Jenkyns (1976), Cretaceous oceanic anoxic events: Causes and consequences, *Geol. Mijnbouw*, *55*, 179–184.
Scholz, F., J. McManus, A. C. Mix, C. Hensen, and R. R. Schneider (2014), The impact of ocean deoxygenation on iron release from continental margin sediments, *Nat. Geosci.*, *7*, 433–437, doi:10.1038/ngeo2162.
Scotese, C. R. (2001), *Atlas of Earth History 1, PALEOMAP Project*, Arlington, Tex.
Scott, C., and T. W. Lyons (2012), Contrasting molybdenum cycling and isotopic properties in euxinic versus non-euxinic sediments and sedimentary rocks: Refining the paleoproxies, *Chem. Geol.*, *324–325*, 19–27, doi:10.1016/j.chemgeo.2012.05.012.
Shipboard Scientific Party (1977), Site 367, in *Deep Sea Drilling Project Initial Report*, edited by Y. Lancelot et al., vol. 41, pp. 163–232, U.S. Gov. Print. Off., Washington, D. C.
Shipboard Scientific Party (1987a), Site 603, in *Deep Sea Drilling Project Initial Report*, edited by J. E. van Hinte, vol. 93, pp. 25–276, U.S. Gov. Print. Off., Washington, D. C.
Shipboard Scientific Party (1987b), Site 641, in *Ocean Drilling Project Initial Report*, edited by G. Boillot et al., vol. 103, pp. 571–649, U.S. Gov. Print. Off., Washington, D. C.
Shipboard Scientific Party (2004), Site 1276, in *Ocean Drilling Project Initial Report*, edited by B. E. Tucholke et al., vol. 210, pp. 1–358, U.S. Gov. Print. Off., Washington, D. C.
Sinninghe Damsté, J. S., and J. Köster (1998), A euxinic southern North Atlantic Ocean during the Cenomanian/Turonian oceanic anoxic event, *Earth Planet. Sci. Lett.*, *158*, 165–173, doi:10.1016/S0012-821X(98)00052-1.
Sinninghe Damsté, J. S., M. M. M. Kuypers, R. D. Pancost, and S. Schouten (2008), The carbon isotopic response of algae, (cyano)bacteria, archaea and higher plants to the late Cenomanian perturbation of the global carbon cycle: Insights from biomarkers in black shales from the Cape Verde Basin (DSDP Site 367), *Org. Geochem.*, *39*, 1703–1718, doi:10.1016/j.orggeochem.2008.01.012.
Sinninghe Damsté, J. S., E. C. van Bentum, G. J. Reichart, J. Pross, and S. Schouten (2010), A CO_2 decrease-driven cooling and increased latitudinal temperature gradient during the mid-Cretaceous Oceanic Anoxic Event 2, *Earth Planet. Sci. Lett.*, *293*, 97–103, doi:10.1016/j.epsl.2010.02.027.
Sinninghe Damsté, J. S., S. Schouten, and J. K. Volkman (2014), C_{27}–C neohop-13(18)-enes and their saturated and aromatic derivatives in sediments: Indicators for diagenesis and water column stratification, *Geochim. Cosmochim. Acta*, *133*, 402–421, doi:10.1016/j.gca.2014.03.008.
Snow, L. J., R. A. Duncan, and T. J. Bralower (2005), Trace element abundances in the Rock Canyon Anticline, Pueblo, Colorado, marine sedimentary section and their relationship to Caribbean plateau construction and oxygen anoxic event 2, *Paleoceanography*, *20*, PA3005, doi:10.1029/2004PA001093.
Takashima, R., H. Nishi, T. Yamanaka, T. Tomosugi, A. G. Fernando, K. Tanabe, K. Moriya, F. Kawabe, and K. Hayashi (2011), Prevailing oxic environments in the Pacific Ocean during the mid-Cretaceous Oceanic Anoxic Event 2, *Nat. Commun.*, *2*, 234, doi:10.1038/ncomms1233.
Taylor, S. R., and S. M. McLennan (1995), The geochemical evolution of the continental crust, *Rev. Geophys.*, *33*, 241–265, doi:10.1029/95RG00262.
Thomson, J., N. C. Higgs, T. R. S. Wilson, I. W. Croudace, G. J. De Lange, and P. J. M. Van Santvoort (1995), Redistribution and geochemical behaviour of redox-sensitive elements around S1, the most recent eastern Mediterranean sapropel, *Geochim. Cosmochim. Acta*, *59*, 3487–3501, doi:10.1016/0016-7037(95)00232-O.
Thurow, J. W., M. Moullade, H.-J. Brumsack, E. Masure, J. Taugourdou, and K. Dunham (1988), The Cenomanian-Turonian Boundary Event (CTBE) at Leg 103/Hole 641, *Proc. Ocean Drill. Program Sci. Results*, *103*, 587–634.

Trabucho Alexandre, A. J., E. Tuenter, G. A. Henstra, K. J. van der Zwan, R. S. W. van de Wal, H. A. Dijkstra, and P. L. de Boer (2010), The mid-Cretaceous North Atlantic nutrient trap: Black shales and OAEs, *Paleoceanography*, *25*, PA4201, doi:10.1029/2010PA001925.

Tsikos, H., et al. (2004), Carbon-isotope stratigraphy recorded by the Cenomanian–Turonian Oceanic Anoxic Event: Correlation and implications based on three key localities, *J. Geol. Soc.*, *161*, 711–719, doi:10.1144/0016-764903-077.

Tucholke, B. E., and P. R. Vogt (1979), Western North Atlantic: Sedimentary evolution and aspects of tectonic history, *Initial Rep. Deep Sea Drill. Proj.*, *43*, 791–825.

Turgeon, S. C., and R. A. Creaser (2008), Cretaceous oceanic anoxic event 2 triggered by a massive magmatic episode, *Nature*, *454*, 323–326, doi:10.1038/nature07076.

Urquhart, E., S. Gardin, R. M. Leckie, S. A. Wood, J. Pross, M. D. Georgescu, B. Ladner, and H. Takata (2007), A paleontological synthesis of ODP Leg 210, Newfoundland Basin, *Proc. Ocean Drill. Program Sci. Results*, *210*, 1–53, doi:10.2973/odp.proc.sr.210.115.

van Bentum, E. C., A. Hetzel, H.-J. Brumsack, A. Forster, G.-J. Reichart, and J. S. Sinninghe Damsté (2009), Reconstruction of water column anoxia in the equatorial Atlantic during the Cenomanian–Turonian oceanic anoxic event using biomarker and trace metal proxies, *Palaeogeogr. Palaeoclimatol. Palaeoecol.*, *280*, 489–498, doi:10.1016/j.palaeo.2009.07.003.

van Bentum, E. C., G.-J. Reichart, and J. S. Sinninghe Damsté (2012), Organic matter provenance, palaeoproductivity and bottom water anoxia during the Cenomanian/Turonian oceanic anoxic event in the Newfoundland Basin (northern proto North Atlantic Ocean), *Org. Geochem.*, *50*, 11–18, doi:10.1016/j.orggeochem.2012.05.013.

van Helmond, N. A. G. M., A. Sluijs, G.-J. Reichart, J. S. Sinninghe Damsté, C. P. Slomp, and H. Brinkhuis (2014), A perturbed hydrological cycle during Oceanic Anoxic Event 2, *Geology*, *42*, 123–126, doi:10.1130/G34929.1.

Westermann, S., M. Caron, N. Fiet, D. Fleitmann, V. Matera, T. Adatte, and K. B. Föllmi (2010), Evidence for oxic conditions during oceanic anoxic event 2 in the northern Tethyan pelagic realm, *Cretaceous Res.*, *31*(5), 500–514, doi:10.1016/j.cretres.2010.07.001.

Westermann, S., M. Stein, V. Matera, N. Fiet, D. Fleitmann, T. Adatte, and K. B. Föllmi (2013), Rapid changes in the redox conditions of the western Tethys Ocean during the early Aptian oceanic anoxic event, *Geochim. Cosmochim. Acta*, *121*, 467–486, doi:10.1016/j.gca.2013.07.023.